5th International Symposium on Particle Image Velocimetry
Busan, Korea, September 22-24, 2003

Time Resolved Stereoscopic PIV in Pipe Flow. Visualizing 3D Flow Structures

C.W.H. van Doorne[1], B. Hof[1], R.H. Lindken[1], J. Westerweel[1]
U. Dierksheide[2]

Abstract

A high speed stereoscopic PIV system (HS-SPIV) was used to study the 3D flow field and flow structures of a puff (turbulent spot) in a pipe. The high sampling frequency of the PIV system allows us to reconstruct 3D velocity fields applying the Taylor-hypothesis. Making 3D plots of iso-contours of the streamwise vorticity, and making various cuts of the 3D vector fields, we have been able to visualize streamwise vortices and low speed streaks. The structural information is extremely valuable in understanding transition to turbulence in pipe flow.

1 Introduction

The performance of a digital PIV system depends largely on the performance of its main components: a laser to illuminate particles in the flow, a digital camera to capture the particle images and a computer to store and evaluate the PIV images. All three components are continuously improved by industry. As a consequence, the field of application of PIV extends with each new generation of PIV systems.

We have used a state-of-the-art high speed stereoscopic PIV (HS-SPIV) system to measure the 3D flow field of a puff (turbulent spot at low Re) in a pipe. The high measurement frequency of the CMOS cameras (1280×1024 px and 500 fps) and a powerful high speed pulsed Nd:YLF laser, make it possible to fully resolve the temporal evolution of t urbulent pipe flow, up to a Re of 6 000 for our pipe flow facility. The HS-PIV system is a follow up of the SPIV system developed by van Doorne, Westerweel & Nieuwstadt [7], with the light sheet oriented perpendicular to the pipe axis. The reason for such orientation of the light sheet was the desire to measure the streamwise vortices, which play an important role in the transition process in a pipe, as found in DNS simulations of Ma *et al.* [4]. With the HS-SPIV system we can take full advantage of the out-of-plane flow orientation. Since the radial and azimuthal velocity components in the central part of the pipe are much smaller than the axial velocity component, we can, in a first approximation, reconstruct the spatial structure of the flow from the time resolved measurements using the Taylor-hypothesis.

The reconstructed 3D flow field is visualized by 3D plots of iso-contours of streamwise vorticity, and various cuts of the 3D vector field.

[1]J.M. Burgers Centre, Delft University of Technology, Leeghwaterstraat 21, 2628 CA Delft, the Netherlands
[2]LaVision GmbH, Anna-Vandenhoeck-Ring 19, D-37081, Goettingen,Germany.

2 Theoretical background

The transition from laminar to turbulent pipe flow is still far from being understood. One of the difficulties is that the laminar parabolic velocity profile is linearly stable, which means that transition must start from a flow disturbance with finite amplitude, although the disturbance may have any form. A sufficiently large and continuous perturbation will lead to a continuous turbulent flow in the pipe for $\mathrm{Re} \gtrsim 2\,600$, and for $\mathrm{Re} \lesssim 1\,800$ all perturbations will eventually decay.

For flow in the intermediate range of $1\,800 \lesssim \mathrm{Re} \lesssim 2\,600$, there will be coexisting laminar and turbulent flow regions, even for very large initial perturbations. The turbulent regions are called 'puffs' (Wygnanski & Champagne [12]). For $\mathrm{Re} \approx 2\,200$ the puff is in an equilibrium with its surrounding laminar flow (Wygnanki *et al.* [11]). The so-called equilibrium-puff does neither grow, nor shrink and travels downstream trough the pipe at a velocity slightly below the bulk velocity ($U_{\mathrm{puff}} \approx 0.9 U_{\mathrm{bulk}}$). At the upstream end of the puff there is a nett flow of laminar fluid entering the turbulent region, and therefore a continuous transition from laminar to turbulent flow occurs at this location. At the downstream end of the puff, the opposite process takes place. Turbulent fluid from the puff re-laminarises and leaves the puff.

A puff represents a minimal flow unit for turbulent pipe flow, i.e. the smallest volume in which a chaotic flow can be sustained given the Re. The flow dynamics in a puff seems therefore a good starting point for understanding turbulence (in a pipe). Furthermore, it may be anticipated that the dynamics of the continuous transition and the upstream side of a puff is also relevant for the transition at larger Re.

3 Experimental setup and procedures

In this section we describe the experimental setup and measurement procedure. An overview of the experimental parameters is presented in table 1, and a sketch of the SPIV system and the coordinate system is shown in figure 1. The High-Speed-Stereoscopic PIV (HS-SPIV) system used in this study is *identical* to the SPIV system described by van Doorne *et al.* [7], with exception of the cameras and the laser.

For our measurements we use a pipe flow facility with an inner diameter of 40 mm and a total length of 28 m. A detailed description of the flow facility is given by Draad [2]. The working fluid is water, and due to a well designed contraction and thermal isolation of the pipe, the flow can be kept laminar up to $\mathrm{Re} = 60\,000$. All measurements were carried out at 26 meters from the inlet.

The PIV images were recorded with two High-Speed-Star-2 cameras from LaVision. The cameras have an 8-bit CMOS sensor with 1280×1024 px (pixel). The maximum image frame rate is 500 Hz, and can be reduced to 250, 125 and 60 Hz. The adjustment of the timing of the laser pulses and camera shutters makes it possible to change the PIV delay time between two subsequent images, just as for contemporary cross-correlation cameras, with a minimum delay time of 8 μs. It is possible to record 1 000 frames, which corresponds to a recording time of 2 seconds at the maximum frame rate. The frequency of the cameras can be further increased at the cost of a reduced image format (e.g., 16 kHz for 32×320 px). Both cameras look at an angle of 45 degrees to the object plane and satisfy the Scheimpflug condition. The cameras are placed in the forward scattering direction of the laser light and therefore stand on different sides of the light sheet (Willert [10]).

Sphericel particles with a nominal diameter of 10 μm were added to the water to increase the particle density. A substantial part of the particles remains in

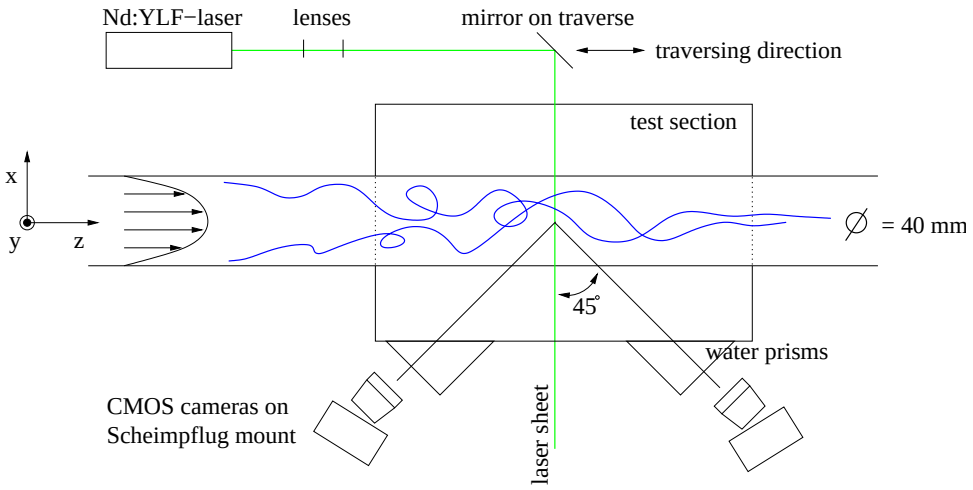

Figure 1: Schematic of High Speed Stereoscopic-PIV system. The coordinate system is also indicated in the graph.

Table 1: Overview of relevant parameters of the experimental setup.

Pipe	diameter	40	mm
	length	30	m
	wall thickness	1.6	mm
Flow	fluid	water	
	Reynolds number	2000	
	bulk velocity	50	mm/s
Seeding	type	Sphericle	
	diameter	10	μm
Light sheet	laser type	Nd:YLF	
	maximum energy	10	mJ/puls
	thickness	1.5	mm
Recording	camera type	CMOS	
	viewing angle	45	degrees
	resolution	1280×1024	px
	frame rate	125	Hz
	lens focal length	105	mm
	f-number	2.8	
	image magnification	0.35	
	viewing area	40×45	mm^2
	exposure delay time	4	ms
	maximum particle displacement	8	px
Interrogation	method	3D calibration	
	interrogation area	32×32	px
	interrogation area	1.4×1.4	mm^2
	resolution with 50% overlap	0.7×0.7	mm^2

suspension, and makes it possible to measure in both laminar and transitional flows.

The flow is illuminated by a pulsed dual-cavity DPPS Nd:YLF laser with a maximum energy of 10 mJ per pulse per laser head at a repetition rate of 1000 Hz (New Wave Pegasus-PIV-30W). The laser beam diameter is approximately 1.5 mm and the wavelength of the light is 527 nm. The light sheet is formed with two lenses, and a mirror on a micro traverse makes it possible to adjust the position of the light sheet.

To minimize optical distortion of the image, the pipe inside the test section is replaced by a 1.6 mm thick glass tube and two water prisms are placed in front of the test section (Prasad 2000).

The light sheet is perpendicular to the mean flow direction in order to capture the flow over the entire cross-section of the pipe and to be able to reconstruct the 3D velocity field from the recorded time sequence. The light sheet thickness has a direct influence on the accuracy of the velocity measurements (van Doorne *et al.* [7]). We used a light sheet thickness of approximately 1.5 mm, which is a good compromise between the spatial resolution and the signal-to-noise ratio. Particle displacements of up to 8 pixels (0.45 mm) result in a strong correlation, and we can resolve displacements with a precision of 0.1 pixel.

The reconstruction of the 3C-vector fields from the two displacement fields of the cameras is based on a 3D calibration of the SPIV system (Soloff *et al.* [6], Prasad [5]). The calibration grid is recorded at two z-positions (instead of one for a 2D calibration), and the method does not require the input of any geometric parameter of the setup.

The data acquisition system is a commercial system from LaVision including the software (Davis 6.3.1) for the evaluation of the vector fields. The vector analysis is done in two steps. In the first step we use 32×32-pixel fixed interrogation windows, after which spurious vectors were detected with a median filter (Westerweel [8]) and replaced by either a vector of a lower correlation peak or an interpolation of the neighboring vectors. In the second step we also used 32×32-pixel interrogation regions, and the vector fields of the first step are used for pre-shifting (Westerweel *et al.* [9]). Again spurious vectors are removed and, if possible, replaced by a vector from a lower correlation peak; spurious vectors are not replaced by interpolated data. After this the vector fields of both cameras are dewarped and recombined (using the 3D calibration) to obtain the 3C-vector field.

For a discussion of details such as the applied calibration grid, the calibration procedure and the procedure to align the laser sheet with the calibration plane, to eliminate the effects of the registration error, we refer to the paper by van Doorne *et al.* [7]. They performed a detailed analysis of the accuracy of the SPIV system with a large out of plane motion. It was found that the SPIV system was able to measure the velocity with high accuracy over the entire cross-section of the pipe. The noise level of individual vectors was smaller than 0.1 px and the turbulence statistics were in excellent agreement with those of the DNS computations by Eggels *et al.* [3]. These experiments were repeated with the HS-SPIV system, and identical results were found.

4 Results

All the results that will be presented in this section are based on a single measurement of a puff at $\mathrm{Re} = 2\,000$. The results will illustrate some of the new possibilities offered by the high speed PIV measurements.

The camera frame rate used for this experiment was 125 Hz, which gave us a measurement time of 8 s. Because the PIV-delay-time was set to 4 ms, the actual measurement frequency was 62.5 Hz. We did not use the maximum camera speed

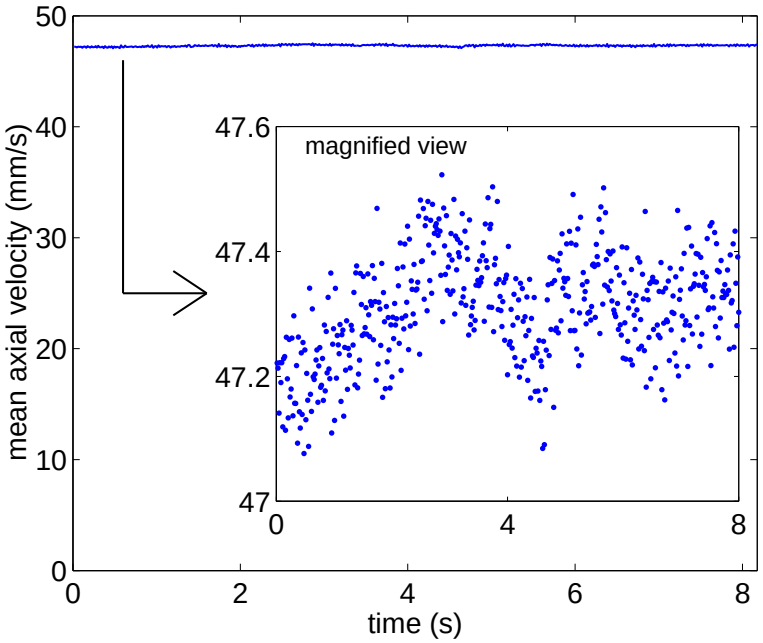

Figure 2: Mean axial velocity averaged over the pipe cross-section as a function of time.

(500 Hz) because the corresponding measurement time of 2 s was too short to capture the entire passage of the puff, which takes about 10 s.

Two results that confirm the accuracy of the measurement equipment are the graphs of the bulk velocity (figure 2) and the probability density functions (PDF) of the three velocity components (figures 3 and 4). The bulk velocity is calculated as the average axial velocity over the cross-section of the pipe. The mean bulk velocity is 47.3 mm/s and the root mean square (rms) of the bulk velocity is 0.085 mm/s, which is 0.18% of the mean bulk velocity. From the trend in the graph we can see that there was a small change in the flow rate due to pump fluctuations and therefore the measurement uncertainty in the flow rate is estimated to be slightly smaller than 0.18%.

The PDFs in figure 3 show a small asymmetry in the measurement of the u_x and the u_y velocity components (from now on referred to as the in-plane velocity components). From the symmetry of the pipe flow one would expect that the two PDFs are identical. A possible explanation is that the PIV-interrogation noise in u_y is about 0.7 ($\sim \frac{1}{2}\sqrt{2}$) smaller than the noise in u_x, because it is the average of two independent measurements of camera 1 and camera 2 (Prasad [5], van Doorne *et al.* [7]). The PDF of u_z in figure 4 shows a small degree of peak-locking to integer pixel values. Furthermore it can be seen that the occurrence of small velocities is somewhat overestimated, which is due to an underestimation of the axial velocity and an increased noise level in the near wall region, caused by bright tracer particles attached to the wall.

The time trace of the axial velocity at the centerline of the pipe is shown in figure 5. We have captured the active region of the puff, around the trailing edge which is located at about 6 s. This is only a part of the full *signature* of a puff as it is known in literature (Wygnanski & Champagne [12], Darbyshire & Mullin [1]). The gradual decrease of the centerline velocity (the leading edge) that is often shown precedes the beginning of our measurement. The leading edge is the region where the flow re-laminarises, and the laminar profile is restored by the growth of the

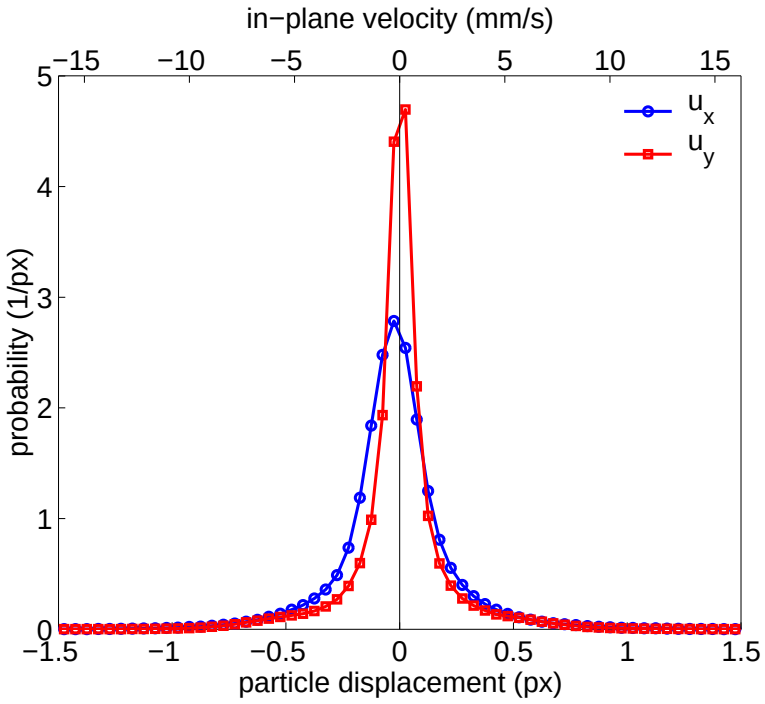

Figure 3: Probability density function of the in-plane velocity components as measured over the entire passage of the puff.

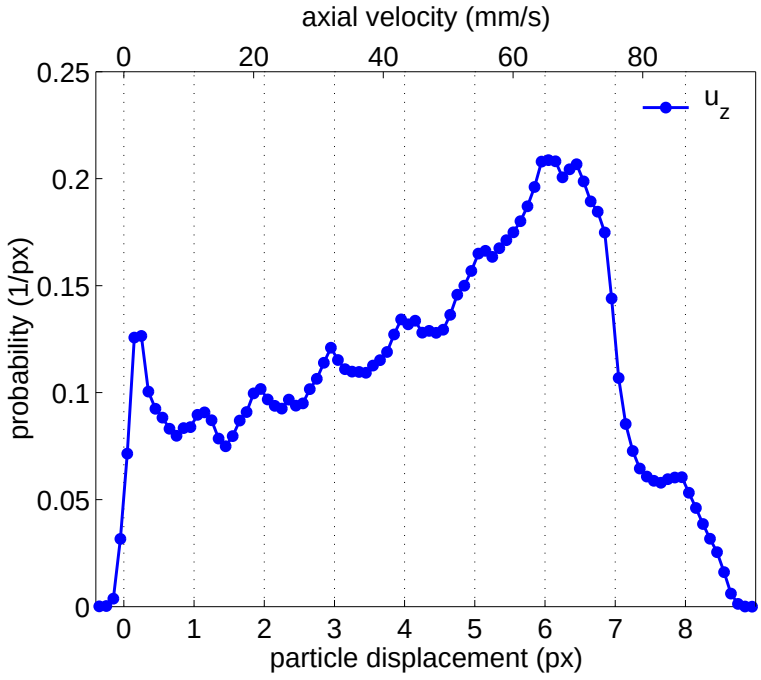

Figure 4: Probability density function of the axial velocity.

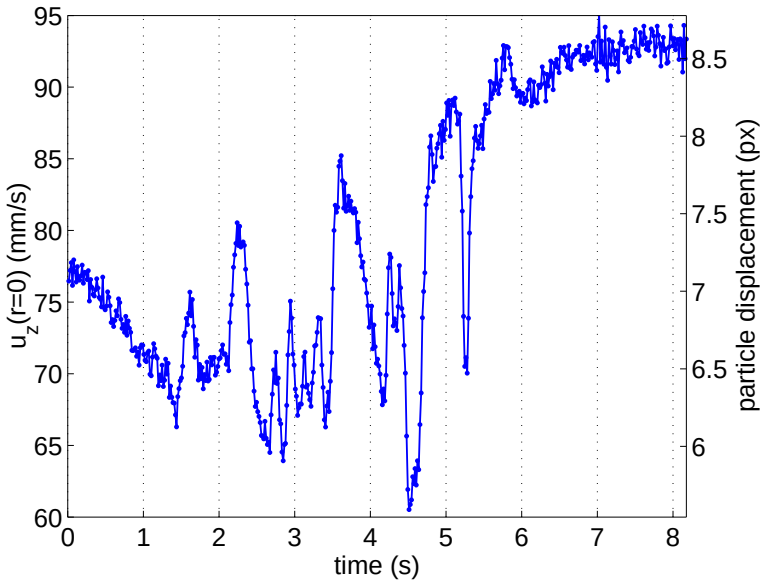

Figure 5: Axial velocity on the center line of the pipe.

boundary layers from the wall. From a dynamical point of view this region is of little interest. An indication of the noise level is given by the right end of the graph, for $t > 6$ s. The flow is laminar in this region (upstream from the puff) and the rapid fluctuations are due to the PIV interrogation noise of the order of 0.1 px.

Figure 6 shows the kinetic energy of the in-plane velocity and it can be seen that the flow has indeed relaminarised upstream of the beginning of our measurement. The kinetic energy of the in-plane velocity is calculated as the mean value of $\langle u_x^2 + u_y^2 \rangle$ over the cross-section of the pipe. Several interesting points can be observed. First of all, there is a very large and sharp peak in the kinetic energy of the in-plane velocity. At conventional sampling rates of 7 or 15 Hz, this peak would not have been properly resolved and might have been rejected as noise. Figure 8(c) shows the in-plane velocity field that corresponds to the peak in the kinetic energy. A very strong cross-flow extends over almost the entire cross-section of the pipe, and a remarkable feature is the highly symmetric configuration of the streamwise vorticity. Further investigation might reveal the relevance and/or dynamics of such vigorous and isolated mixing of the flow.

Another interesting point is the rapid increase of the total kinetic energy for $t > 6$ s (figure 7). In order to understand the transition it may be useful to study the flow in an Lagrangian frame of reference that moves with the fluid. Laminar fluid initially upstream of the puff continuously enters the puff and undergoes transition to turbulence. Traveling with the fluid, we should thus read the figure from right to left. We then see that subststantial fracion of the kinetic energy of the streamwise velocity will be lost (due to changes in the mean profile), even before the flow has become fully turbulent and the turbulence could have increased the dissipation of the kinetic energy. We find this quite surprising, and this might indicate that the pressure plays an important role in the energy redistribution in this region. These speculations of course will be subject of further investigations.

A 3D visualization of the iso-surfaces of the streamwise vorticity in the puff is shown in figure 9. Since the velocity fluctuations are much smaller than the mean downstream velocity, we can, in a first approximation, apply the Taylor hypothesis to convert time into space. The z-coordinate has actually been calculated by multi-

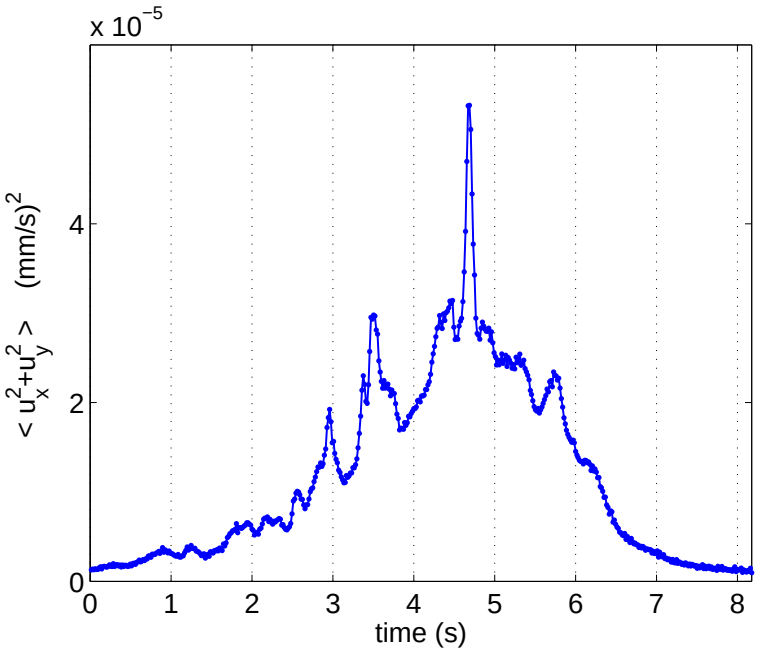

Figure 6: Kinetic energy of the in-plane velocity.

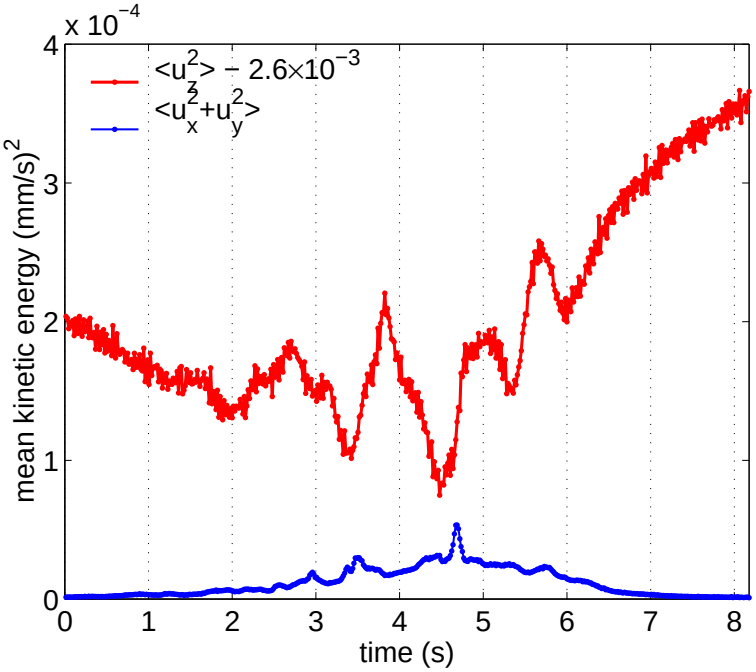

Figure 7: Kinetic Energy of the in-plane and axial velocity

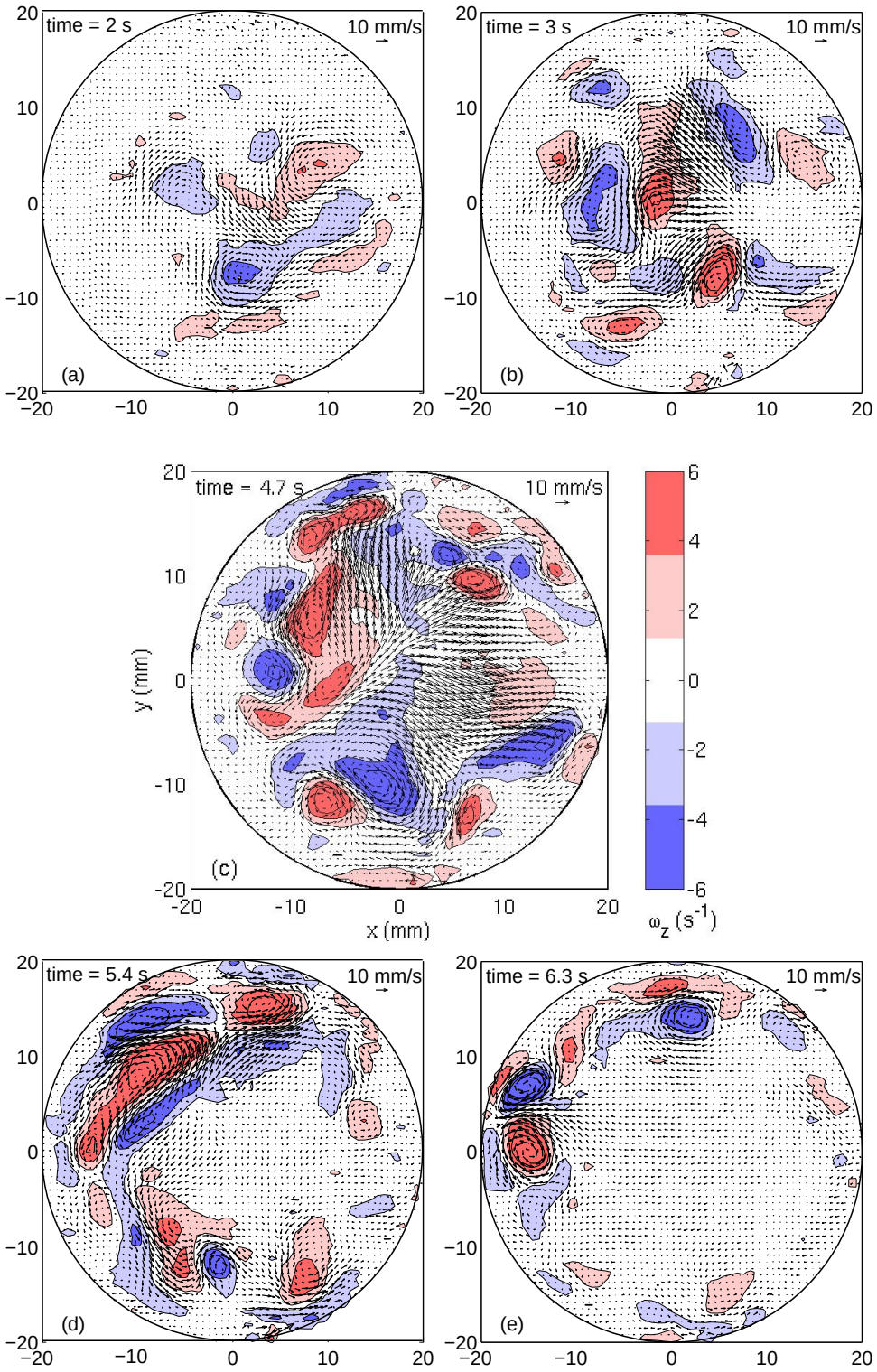

Figure 8: Inplane velocity fields and axial vorticity at different instance of time. Sub-figure c is at the moment of maximal in-plane kinetic energy, see figure 6.

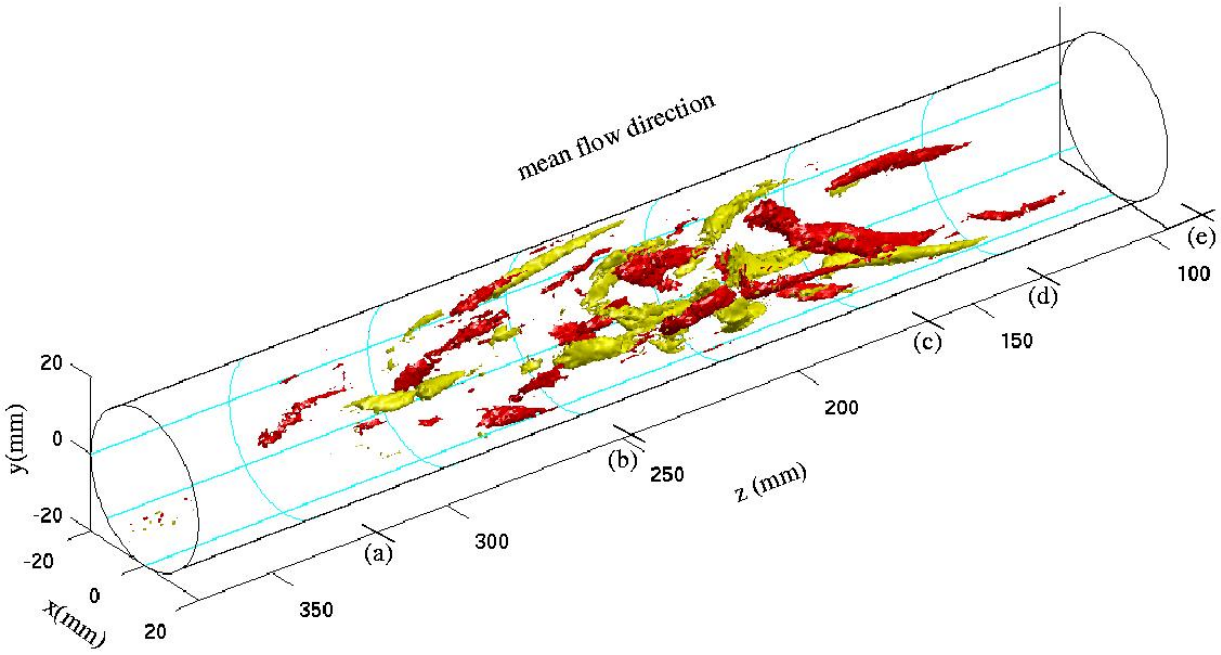

Figure 9: 3D visualization of the iso-contours of streamwise vorticity ($\pm$ 5.5 s^{-1}) in the puff. The letters on the z-axis refere to the sub-figures of figure 8.

plication of the measurement time and bulk velocity. The flow structures visualized in the reconstructed 3D flow field may not have the exact shape and orientation as in the real flow, but we expect the qualitative picture to be correct.

From figures 8 and 9, and from movies that were not presented in this paper, it appears that the transition at the upstream end of the puff starts with the appearance of weak low speed streaks and streamwise vortices close to the wall. The streaks and vortices grow and eventually breakdown to result in a turbulent flow. The appearance of the first streaks and streamwise vortices is rather chaotically distributed along the circumference of the pipe. So far we have not been able to find any clear organization in the late stages of the transition and the interior of the puff. Even at these very low Re the flow dynamics of the transition is very complicated and chaotic.

5 Conclusion and discussion

A state of the art high speed stereoscopic PIV (HS-SPIV) system was used for the study of laminar turbulent transition in a puff in pipe flow. The HS-SPIV system has the same accuracy as a conventional SPIV system. The high sampling rate has made it possible to fully resolve the temporal evolution of the flow (at 500 Hz up to Re = 6 000 for our setup) and access complicated quantities such as the time evolution of the kinetic energy.

The 3D flow field of a puff was reconstructed from the time resolved measurements by application of the Taylor-hypothesis to convert time to space. In particular this measurement revealed a large spike in the kinetic energy. At conventional sampling rates of 7 or 15 Hz, this spike would probably not have been discovered. The streamwise vortices were visualized by means of a 3D plot of the iso-contours of the

vorticity.

We conclude that the high speed SPIV technique applied to a cross-flow can measure 3D flow fields and reveal its 3D flow structure, which so far was only possible with (DNS) calculations.

In the near future we will further explore the data set of several other puffs that were recorded at different Re. Measurements at 500 Hz were also performed for fully developed turbulent flow at Re = 3 000 and Re = 5 300 and for turbulent flow with drag reducing polymers. We also plan to extract the 3D vorticity vector field from the 3D velocity fields.

References

[1] A.G. Darbyshire and T. Mullin. Transition to turbulence in constant-mass-flux pipe flow. *J. Fluid Mech.*, 289:83–114, 1995.

[2] A.A. Draad. *Laminar-turbulent transition in pipe flow for Newtonian and non-Newtonian fluids*. PhD thesis, Delft Universtity of Technology, 1998.

[3] J.G.M. Eggels, J. Westerweel, and F.T.M. Nieuwstadt. Direct numerical simulation of turbulent pipe flow. *Appl. Sci. Res.*, 51:319–324, 1993.

[4] B. Ma, C.W.H. Doorne, Z. Zhang, and F.T.M. Nieuwstadt. On the spatial evolution of a wall-imposed periodic disturbance in pipe poiseuille flow at $re = 3000$. part1. sub-critical disturbance,. *J. Fluid Mech.*, 398:181–224, 1999.

[5] A.K. Prasad. Stereoscopic particle image velocimetry. *Exp. Fluids*, 29:103–116, 2000.

[6] S.M. Soloff, R.J. Adrian, and Z.C. Liu. Distortion compensation for generalised stereoscopic particle image velocimetry. *Meas. Sci. Technol.*, 8:1441–1454, 1997.

[7] C.W.H. van Doorne, J. Westerweel, and F.T.M. Nieuwstadt. Measurement uncertainty of stereoscopic-piv for flow with large out-of-plane motion. In *Proceedings of the EUROPIV 2 final workshop on Particle Image Velocimetry, Zaragoza, Spain*. Springer Verlag, 2003.

[8] J. Westerweel. Efficient detection of spurious vectors in particle image velocimetry data. *Exp. Fluids*, 16:236–247, 1994.

[9] J. Westerweel, D. Dabiri, and M. Gharib. The effect to a discrete window offset on the accuracy of cross-correlation analysis of digital piv recordings. *Exp. Fluids*, 23:20–28, 1997.

[10] C. Willert. Stereoscopic digital particle image velocimetry for application in wind tunnel flows. *Meas. Sci. Technol.*, 8:1465–1479, 1997.

[11] I. Wygnanski, M. Sokolov, and D. Friedman. On transition in a pipe. part 2. the equilibrium puff. *J. Fluid Mech.*, 69:283–304, 1975.

[12] I.J. Wygnanski and F.H. Champagne. On transition in a pipe. part 1. the origin of puffs and slugs and the flow in a turbulent slug. *J. Fluid Mech.*, 59:281–335, 1973.